BABAR-PUB-14/002
SLAC-PUB-15979
arXiv:1406.2980 [hep-ex]

Search for a dark photon in e^+e^- collisions at *BABAR*

J. P. Lees,[1] V. Poireau,[1] V. Tisserand,[1] E. Grauges,[2] A. Palano[ab],[3] G. Eigen,[4] B. Stugu,[4] D. N. Brown,[5] M. Feng,[5] L. T. Kerth,[5] Yu. G. Kolomensky,[5] M. J. Lee,[5] G. Lynch,[5] H. Koch,[6] T. Schroeder,[6] C. Hearty,[7] T. S. Mattison,[7] J. A. McKenna,[7] R. Y. So,[7] A. Khan,[8] V. E. Blinov[abc],[9] A. R. Buzykaev[a],[9] V. P. Druzhinin[ab],[9] V. B. Golubev[ab],[9] E. A. Kravchenko[ab],[9] A. P. Onuchin[abc],[9] S. I. Serednyakov[ab],[9] Yu. I. Skovpen[ab],[9] E. P. Solodov[ab],[9] K. Yu. Todyshev[ab],[9] A. J. Lankford,[10] M. Mandelkern,[10] B. Dey,[11] J. W. Gary,[11] O. Long,[11] C. Campagnari,[12] M. Franco Sevilla,[12] T. M. Hong,[12] D. Kovalskyi,[12] J. D. Richman,[12] C. A. West,[12] A. M. Eisner,[13] W. S. Lockman,[13] W. Panduro Vazquez,[13] B. A. Schumm,[13] A. Seiden,[13] D. S. Chao,[14] C. H. Cheng,[14] B. Echenard,[14] K. T. Flood,[14] D. G. Hitlin,[14] T. S. Miyashita,[14] P. Ongmongkolkul,[14] F. C. Porter,[14] R. Andreassen,[15] Z. Huard,[15] B. T. Meadows,[15] B. G. Pushpawela,[15] M. D. Sokoloff,[15] L. Sun,[15] P. C. Bloom,[16] W. T. Ford,[16] A. Gaz,[16] J. G. Smith,[16] S. R. Wagner,[16] R. Ayad,[17,*] W. H. Toki,[17] B. Spaan,[18] D. Bernard,[19] M. Verderi,[19] S. Playfer,[20] D. Bettoni[a],[21] C. Bozzi[a],[21] R. Calabrese[ab],[21] G. Cibinetto[ab],[21] E. Fioravanti[ab],[21] I. Garzia[ab],[21] E. Luppi[ab],[21] L. Piemontese[a],[21] V. Santoro[a],[21] A. Calcaterra,[22] R. de Sangro,[22] G. Finocchiaro,[22] S. Martellotti,[22] P. Patteri,[22] I. M. Peruzzi,[22,†] M. Piccolo,[22] M. Rama,[22] A. Zallo,[22] R. Contri[ab],[23] M. Lo Vetere[ab],[23] M. R. Monge[ab],[23] S. Passaggio[a],[23] C. Patrignani[ab],[23] E. Robutti[a],[23] B. Bhuyan,[24] V. Prasad,[24] A. Adametz,[25] U. Uwer,[25] H. M. Lacker,[26] P. D. Dauncey,[27] U. Mallik,[28] C. Chen,[29] J. Cochran,[29] S. Prell,[29] H. Ahmed,[30] A. V. Gritsan,[31] N. Arnaud,[32] M. Davier,[32] D. Derkach,[32] G. Grosdidier,[32] F. Le Diberder,[32] A. M. Lutz,[32] B. Malaescu,[32,‡] P. Roudeau,[32] A. Stocchi,[32] G. Wormser,[32] D. J. Lange,[33] D. M. Wright,[33] J. P. Coleman,[34] J. R. Fry,[34] E. Gabathuler,[34] D. E. Hutchcroft,[34] D. J. Payne,[34] C. Touramanis,[34] A. J. Bevan,[35] F. Di Lodovico,[35] R. Sacco,[35] G. Cowan,[36] J. Bougher,[37] D. N. Brown,[37] C. L. Davis,[37] A. G. Denig,[38] M. Fritsch,[38] W. Gradl,[38] K. Griessinger,[38] A. Hafner,[38] K. R. Schubert,[38] R. J. Barlow,[39,§] G. D. Lafferty,[39] R. Cenci,[40] B. Hamilton,[40] A. Jawahery,[40] D. A. Roberts,[40] R. Cowan,[41] G. Sciolla,[41] R. Cheaib,[42] P. M. Patel,[42,¶] S. H. Robertson,[42] N. Neri[a],[43] F. Palombo[ab],[43] L. Cremaldi,[44] R. Godang,[44,**] P. Sonnek,[44] D. J. Summers,[44] M. Simard,[45] P. Taras,[45] G. De Nardo[ab],[46] G. Onorato[ab],[46] C. Sciacca[ab],[46] M. Martinelli,[47] G. Raven,[47] C. P. Jessop,[48] J. M. LoSecco,[48] K. Honscheid,[49] R. Kass,[49] E. Feltresi[ab],[50] M. Margoni[ab],[50] M. Morandin[a],[50] M. Posocco[a],[50] M. Rotondo[a],[50] G. Simi[ab],[50] F. Simonetto[ab],[50] R. Stroili[ab],[50] S. Akar,[51] E. Ben-Haim,[51] M. Bomben,[51] G. R. Bonneaud,[51] H. Briand,[51] G. Calderini,[51] J. Chauveau,[51] Ph. Leruste,[51] G. Marchiori,[51] J. Ocariz,[51] M. Biasini[ab],[52] E. Manoni[a],[52] S. Pacetti[ab],[52] A. Rossi[a],[52] C. Angelini[ab],[53] G. Batignani[ab],[53] S. Bettarini[ab],[53] M. Carpinelli[ab],[53,††] G. Casarosa[ab],[53] A. Cervelli[ab],[53] M. Chrzaszcz[a],[53] F. Forti[ab],[53] M. A. Giorgi[ab],[53] A. Lusiani[ac],[53] B. Oberhof[ab],[53] E. Paoloni[ab],[53] A. Perez[a],[53] G. Rizzo[ab],[53] J. J. Walsh[a],[53] D. Lopes Pegna,[54] J. Olsen,[54] A. J. S. Smith,[54] R. Faccini[ab],[55] F. Ferrarotto[a],[55] F. Ferroni[ab],[55] M. Gaspero[ab],[55] L. Li Gioi[a],[55] A. Pilloni[ab],[55] G. Piredda[a],[55] C. Bünger,[56] S. Dittrich,[56] O. Grünberg,[56] T. Hartmann,[56] M. Hess,[56] T. Leddig,[56] C. Voß,[56] R. Waldi,[56] T. Adye,[57] E. O. Olaiya,[57] F. F. Wilson,[57] S. Emery,[58] G. Vasseur,[58] F. Anulli,[59,‡‡] D. Aston,[59] D. J. Bard,[59] C. Cartaro,[59] M. R. Convery,[59] J. Dorfan,[59] G. P. Dubois-Felsmann,[59] W. Dunwoodie,[59] M. Ebert,[59] R. C. Field,[59] B. G. Fulsom,[59] M. T. Graham,[59] C. Hast,[59] W. R. Innes,[59] P. Kim,[59] D. W. G. S. Leith,[59] P. Lewis,[59] D. Lindemann,[59] S. Luitz,[59] V. Luth,[59] H. L. Lynch,[59] D. B. MacFarlane,[59] D. R. Muller,[59] H. Neal,[59] M. Perl,[59] T. Pulliam,[59] B. N. Ratcliff,[59] A. Roodman,[59] A. A. Salnikov,[59] R. H. Schindler,[59] A. Snyder,[59] D. Su,[59] M. K. Sullivan,[59] J. Va'vra,[59] W. J. Wisniewski,[59] H. W. Wulsin,[59] M. V. Purohit,[60] R. M. White,[60,§§] J. R. Wilson,[60] A. Randle-Conde,[61] S. J. Sekula,[61] M. Bellis,[62] P. R. Burchat,[62] E. M. T. Puccio,[62] M. S. Alam,[63] J. A. Ernst,[63] R. Gorodeisky,[64] N. Guttman,[64] D. R. Peimer,[64] A. Soffer,[64] S. M. Spanier,[65] J. L. Ritchie,[66] A. M. Ruland,[66] R. F. Schwitters,[66] B. C. Wray,[66] J. M. Izen,[67] X. C. Lou,[67] F. Bianchi[ab],[68] F. De Mori[ab],[68] A. Filippi[a],[68] D. Gamba[ab],[68] L. Lanceri[ab],[69] L. Vitale[ab],[69] F. Martinez-Vidal,[70] A. Oyanguren,[70] P. Villanueva-Perez,[70] J. Albert,[71] Sw. Banerjee,[71] A. Beaulieu,[71] F. U. Bernlochner,[71] H. H. F. Choi,[71] G. J. King,[71] R. Kowalewski,[71] M. J. Lewczuk,[71] T. Lueck,[71] I. M. Nugent,[71] J. M. Roney,[71] R. J. Sobie,[71] N. Tasneem,[71] T. J. Gershon,[72] P. F. Harrison,[72] T. E. Latham,[72] H. R. Band,[73] S. Dasu,[73] Y. Pan,[73] R. Prepost,[73] and S. L. Wu[73]

SLAC National Accelerator Laboratory, 2575 Sand Hill Road, Menlo Park, CA 94025

This material is based upon work supported by the U.S. Department of Energy, Office of Science, Office of Basic Energy Sciences, under Contract No. DE-AC02-76SF00515 and HEP.

(The *BABAR* Collaboration)

[1]*Laboratoire d'Annecy-le-Vieux de Physique des Particules (LAPP), Université de Savoie, CNRS/IN2P3, F-74941 Annecy-Le-Vieux, France*
[2]*Universitat de Barcelona, Facultat de Fisica, Departament ECM, E-08028 Barcelona, Spain*
[3]*INFN Sezione di Bari[a]; Dipartimento di Fisica, Università di Bari[b], I-70126 Bari, Italy*
[4]*University of Bergen, Institute of Physics, N-5007 Bergen, Norway*
[5]*Lawrence Berkeley National Laboratory and University of California, Berkeley, California 94720, USA*
[6]*Ruhr Universität Bochum, Institut für Experimentalphysik 1, D-44780 Bochum, Germany*
[7]*University of British Columbia, Vancouver, British Columbia, Canada V6T 1Z1*
[8]*Brunel University, Uxbridge, Middlesex UB8 3PH, United Kingdom*
[9]*Budker Institute of Nuclear Physics SB RAS, Novosibirsk 630090[a], Novosibirsk State University, Novosibirsk 630090[b], Novosibirsk State Technical University, Novosibirsk 630092[c], Russia*
[10]*University of California at Irvine, Irvine, California 92697, USA*
[11]*University of California at Riverside, Riverside, California 92521, USA*
[12]*University of California at Santa Barbara, Santa Barbara, California 93106, USA*
[13]*University of California at Santa Cruz, Institute for Particle Physics, Santa Cruz, California 95064, USA*
[14]*California Institute of Technology, Pasadena, California 91125, USA*
[15]*University of Cincinnati, Cincinnati, Ohio 45221, USA*
[16]*University of Colorado, Boulder, Colorado 80309, USA*
[17]*Colorado State University, Fort Collins, Colorado 80523, USA*
[18]*Technische Universität Dortmund, Fakultät Physik, D-44221 Dortmund, Germany*
[19]*Laboratoire Leprince-Ringuet, Ecole Polytechnique, CNRS/IN2P3, F-91128 Palaiseau, France*
[20]*University of Edinburgh, Edinburgh EH9 3JZ, United Kingdom*
[21]*INFN Sezione di Ferrara[a]; Dipartimento di Fisica e Scienze della Terra, Università di Ferrara[b], I-44122 Ferrara, Italy*
[22]*INFN Laboratori Nazionali di Frascati, I-00044 Frascati, Italy*
[23]*INFN Sezione di Genova[a]; Dipartimento di Fisica, Università di Genova[b], I-16146 Genova, Italy*
[24]*Indian Institute of Technology Guwahati, Guwahati, Assam, 781 039, India*
[25]*Universität Heidelberg, Physikalisches Institut, D-69120 Heidelberg, Germany*
[26]*Humboldt-Universität zu Berlin, Institut für Physik, D-12489 Berlin, Germany*
[27]*Imperial College London, London, SW7 2AZ, United Kingdom*
[28]*University of Iowa, Iowa City, Iowa 52242, USA*
[29]*Iowa State University, Ames, Iowa 50011-3160, USA*
[30]*Physics Department, Jazan University, Jazan 22822, Kingdom of Saudia Arabia*
[31]*Johns Hopkins University, Baltimore, Maryland 21218, USA*
[32]*Laboratoire de l'Accélérateur Linéaire, IN2P3/CNRS et Université Paris-Sud 11, Centre Scientifique d'Orsay, F-91898 Orsay Cedex, France*
[33]*Lawrence Livermore National Laboratory, Livermore, California 94550, USA*
[34]*University of Liverpool, Liverpool L69 7ZE, United Kingdom*
[35]*Queen Mary, University of London, London, E1 4NS, United Kingdom*
[36]*University of London, Royal Holloway and Bedford New College, Egham, Surrey TW20 0EX, United Kingdom*
[37]*University of Louisville, Louisville, Kentucky 40292, USA*
[38]*Johannes Gutenberg-Universität Mainz, Institut für Kernphysik, D-55099 Mainz, Germany*
[39]*University of Manchester, Manchester M13 9PL, United Kingdom*
[40]*University of Maryland, College Park, Maryland 20742, USA*
[41]*Massachusetts Institute of Technology, Laboratory for Nuclear Science, Cambridge, Massachusetts 02139, USA*
[42]*McGill University, Montréal, Québec, Canada H3A 2T8*
[43]*INFN Sezione di Milano[a]; Dipartimento di Fisica, Università di Milano[b], I-20133 Milano, Italy*
[44]*University of Mississippi, University, Mississippi 38677, USA*
[45]*Université de Montréal, Physique des Particules, Montréal, Québec, Canada H3C 3J7*
[46]*INFN Sezione di Napoli[a]; Dipartimento di Scienze Fisiche, Università di Napoli Federico II[b], I-80126 Napoli, Italy*
[47]*NIKHEF, National Institute for Nuclear Physics and High Energy Physics, NL-1009 DB Amsterdam, The Netherlands*
[48]*University of Notre Dame, Notre Dame, Indiana 46556, USA*
[49]*Ohio State University, Columbus, Ohio 43210, USA*
[50]*INFN Sezione di Padova[a]; Dipartimento di Fisica, Università di Padova[b], I-35131 Padova, Italy*
[51]*Laboratoire de Physique Nucléaire et de Hautes Energies, IN2P3/CNRS, Université Pierre et Marie Curie-Paris6, Université Denis Diderot-Paris7, F-75252 Paris, France*
[52]*INFN Sezione di Perugia[a]; Dipartimento di Fisica, Università di Perugia[b], I-06123 Perugia, Italy*
[53]*INFN Sezione di Pisa[a]; Dipartimento di Fisica, Università di Pisa[b]; Scuola Normale Superiore di Pisa[c], I-56127 Pisa, Italy*
[54]*Princeton University, Princeton, New Jersey 08544, USA*

[55]INFN Sezione di Roma[a]; Dipartimento di Fisica,
Università di Roma La Sapienza[b], I-00185 Roma, Italy
[56]Universität Rostock, D-18051 Rostock, Germany
[57]Rutherford Appleton Laboratory, Chilton, Didcot, Oxon, OX11 0QX, United Kingdom
[58]CEA, Irfu, SPP, Centre de Saclay, F-91191 Gif-sur-Yvette, France
[59]SLAC National Accelerator Laboratory, Stanford, California 94309 USA
[60]University of South Carolina, Columbia, South Carolina 29208, USA
[61]Southern Methodist University, Dallas, Texas 75275, USA
[62]Stanford University, Stanford, California 94305-4060, USA
[63]State University of New York, Albany, New York 12222, USA
[64]Tel Aviv University, School of Physics and Astronomy, Tel Aviv, 69978, Israel
[65]University of Tennessee, Knoxville, Tennessee 37996, USA
[66]University of Texas at Austin, Austin, Texas 78712, USA
[67]University of Texas at Dallas, Richardson, Texas 75083, USA
[68]INFN Sezione di Torino[a]; Dipartimento di Fisica, Università di Torino[b], I-10125 Torino, Italy
[69]INFN Sezione di Trieste[a]; Dipartimento di Fisica, Università di Trieste[b], I-34127 Trieste, Italy
[70]IFIC, Universitat de Valencia-CSIC, E-46071 Valencia, Spain
[71]University of Victoria, Victoria, British Columbia, Canada V8W 3P6
[72]Department of Physics, University of Warwick, Coventry CV4 7AL, United Kingdom
[73]University of Wisconsin, Madison, Wisconsin 53706, USA

Dark sectors charged under a new Abelian interaction have recently received much attention in the context of dark matter models. These models introduce a light new mediator, the so-called dark photon (A'), connecting the dark sector to the Standard Model. We present a search for a dark photon in the reaction $e^+e^- \to \gamma A', A' \to e^+e^-, \mu^+\mu^-$ using 514 fb^{-1} of data collected with the *BABAR* detector. We observe no statistically significant deviations from the Standard Model predictions, and we set 90% confidence level upper limits on the mixing strength between the photon and dark photon at the level of $10^{-4} - 10^{-3}$ for dark photon masses in the range $0.02 - 10.2\,\mathrm{GeV}$. We further constrain the range of the parameter space favored by interpretations of the discrepancy between the calculated and measured anomalous magnetic moment of the muon.

PACS numbers: 12.60.-i, 14.80.-j, 13.66.Hk, 95.35.+d

Dark sectors, which introduce new particles neutral under the Standard Model (SM) gauge symmetries, arise in many models of physics beyond the Standard Model [1]. These particles would only interact feebly with ordinary matter, and could easily have escaped detection in past experimental searches. Besides gravity, a few renormalizable interactions provide a portal into dark sectors. One of the simplest realizations consists of a dark sector charged under a new gauge group $U(1)'$. The corresponding gauge boson, dubbed the dark photon (A'), couples to the SM hypercharge via kinetic mixing [2] with a mixing strength ϵ. This results in an effective interaction $\epsilon e A'_\mu J^\mu_{EM}$ between the dark photon and the electromagnetic current J^μ_{EM} after electroweak symmetry breaking. This idea has recently received much attention in the context of dark matter models, where weakly interacting massive particles reside in a dark sector charged under a new Abelian interaction [3–5]. Within this framework, dark photons would mediate the annihilation of WIMP particles into SM fermions. To accommodate the recent anomalies observed in cosmic rays [6–8], the dark photon mass is constrained to be in the MeV to GeV range.

Low-energy e^+e^- colliders offer an ideal environment to probe low-mass dark sectors [9, 10]. Dark photons could be produced in association with a photon in e^+e^- collisions, and decay back to SM fermions if other dark sector states are kinematically inaccessible. The dark photon width, suppressed by a factor ϵ^2, is expected to be well below the experimental resolution. Dark photons could therefore be detected as narrow resonances in radiative $e^+e^- \to \gamma l^+l^-$ ($l = e, \mu$) events. No unambiguous signal for a dark photon has been reported so far, and constraints have been set on the mixing strength between the photon and dark photon as a function of the dark photon mass [11–22]. Searches for an additional low-mass, dark gauge boson [23] or dark Higgs boson [24] have also yielded negative results.

We report herein a search for dark photons in the reaction $e^+e^- \to \gamma A', A' \to l^+l^-$ ($l = e, \mu$) with data recorded by the *BABAR* detector [25, 26]. This search is based on 514 fb^{-1} of data collected mostly at the $\Upsilon(4S)$ resonance, but also at the $\Upsilon(3S)$ and $\Upsilon(2S)$ peaks, as well as data in the vicinity of these resonances [27]. We probe dark photon masses in the range $0.02\,\mathrm{GeV} < m_{A'} < 10.2\,\mathrm{GeV}$ [28]. To avoid experimental bias, we examine the data only after finalizing the analysis strategy. About 5% of the dataset is used to optimize the selection criteria and validate the fitting procedure, and is then discarded from the final data sample.

Simulated signal events are generated by MadGraph [29] for 35 different A' mass hypotheses. The background processes $e^+e^- \to e^+e^-(\gamma)$ and $e^+e^- \to$

$\gamma\gamma(\gamma)$ are simulated using BHWIDE [30] (see below), and $e^+e^- \to \mu^+\mu^-(\gamma)$ events are generated with KK [31]. Resonance production processes in initial state radiation, $e^+e^- \to \gamma X$ ($X = J/\psi, \psi(2S), \Upsilon(1S), \Upsilon(2S)$), are simulated using a structure function technique [32, 33]. The detector acceptance and reconstruction efficiencies are determined using a Monte Carlo (MC) simulation based on GEANT4 [34].

We select events containing two oppositely charged tracks and a single photon having a center-of-mass (CM) energy greater than 0.2 GeV. Additional low-energy photons are allowed if their energies measured in the laboratory frame do not exceed 0.2 GeV. At least one track is required to be identified as an electron, or both tracks as muons, by particle identification algorithms. The cosine of the muon helicity angle, defined as the angle between the muon and the CM frame in the A' rest frame, must be less than 0.95. To further suppress the contribution from radiative Bhabha events, we also require the cosine of the polar angle (the angle with respect to the electron beam axis) of the positron in the CM frame to be larger than -0.5, and that of the electron to be less than 0.5. The $\gamma l^+ l^-$ system is then fit, constraining the center-of-mass energy of the candidate to be within the beam energy spread and requiring the tracks to originate from the interaction point to within its spread. Finally, we require the χ^2 of the fit to be less than 30 (for 8 d.o.f). These criteria are chosen to maximize the signal significance over a broad mass range.

A large contribution from converted photons produced in $e^+e^- \to \gamma\gamma, \gamma \to e^+e^-$ events is still present at low e^+e^- invariant mass. A neural network is trained to further reduce this background using the following variables: the flight length of the e^+e^- pair in the plane transverse to the beam, and the corresponding flight significance, the electron helicity angle, the polar angle of the e^+e^- system, and the angle between the photon and the plane formed by the two tracks. We apply a requirement on the neural network output that selects approximately 70% of the signal in the low-mass region, and rejects more than 99.7% of the photon conversions. The uncertainty associated with this selection criterion, estimated from a sample of $\pi^0 \to \gamma e^+e^-$ decays, is at the level of 2% at $m_{A'} \sim 20\,\mathrm{MeV}$, and decreases rapidly to negligible levels above $m_{A'} \sim 50\,\mathrm{MeV}$.

The resulting dielectron and reduced dimuon mass distributions are displayed in Fig. 1, together with the predictions of various simulated SM processes. The reduced dimuon mass, $m_R = \sqrt{m^2_{\mu\mu} - 4m^2_\mu}$, is easier to model near threshold than the dimuon mass. The dielectron (reduced dimuon) mass spectrum is dominated by radiative Bhabha (dimuon) production, with smaller peaking contributions from ISR production of $J/\psi, \psi(2S)$, $\Upsilon(1S)$, and $\Upsilon(2S)$ resonances. The contribution from $\phi \to K^+K^-$, where both kaons are misidentified as electrons or muons, is found to be negligible. The mass distributions are generally well described by the simulation, except in the low e^+e^- mass region, where, as expected, BHWIDE fails to reproduce events in which the two leptons are separated by a small angle. Since the signal extraction procedure does not depend on the background predictions, this disagreement has little impact on the search.

The signal selection efficiency, typically 15% (35%) for the dielectron (dimuon) channel, is determined from Monte Carlo simulation. The difference is mostly due to trigger efficiencies. For electrons, this is lowered in order to suppress the rate of radiative Bhabha events. Correction factors to the efficiency, which vary between 0.5% to 3%, account for the effects of triggers, charged particle identification, and track and photon reconstruction. These are assessed by fitting the ratios of the measured and simulated $e^+e^- \to e^+e^-\gamma$ and $e^+e^- \to \mu^+\mu^-\gamma$ differential mass distributions, as shown in Fig. 1. For the dielectron channel, we fit the ratio only in the region $m_{e^+e^-} > 3\,\mathrm{GeV}$, where the simulation is expected to provide reliable predictions, and extrapolate the corrections to the low-mass region. The entire mass range is used for the dimuon final state. Half of the corrections are propagated as systematic uncertainties to cover statistical variations between neighboring mass points and the uncertainty associated to the extrapolation procedure.

The signal yield as a function of $m_{A'}$ is extracted by performing a series of independent fits to the dielectron and the reduced dimuon mass spectra for each beam energy. The fits are performed in the range $0.02\,\mathrm{GeV} < m_{A'} < 10.2\,\mathrm{GeV}$ ($0.212\,\mathrm{GeV} < m_{A'} < 10.2\,\mathrm{GeV}$) for the dielectron (dimuon) sample taken near the $\Upsilon(4S)$ resonance, and up to 9.6 GeV and 10.0 GeV for the dataset collected near the $\Upsilon(2S)$ and $\Upsilon(3S)$ resonances, respectively [28]. We search for a dark photon in varying mass steps that correspond to approximately half of the dark photon mass resolution. Each fit is performed over an interval at least 20 times broader than the signal resolution at that mass, with the constraint $m_{e^+e^-} > 0.015\,\mathrm{GeV}$ for the dielectron channel. For the purposes of determining the mass steps, the signal resolution is estimated by Gaussian fits to several simulated A' samples, and interpolated to all other masses. It varies between 1.5 and 8 MeV. We sample a total of 5704 (5370) mass hypotheses for the dielectron (dimuon) channel. Example of fits can be found in the supplemental material [35]. The bias in the fitted values is estimated from a large ensemble of pseudo-experiments and found to be negligible.

The likelihood function, described below, contains contributions from signal, radiative dilepton background, and peaking background where appropriate. The signal probability density function (pdf) is modeled directly from the signal Monte Carlo mass distribution using a non-parametric kernel pdf, and interpolated between the known simulated masses using an algorithm based on the

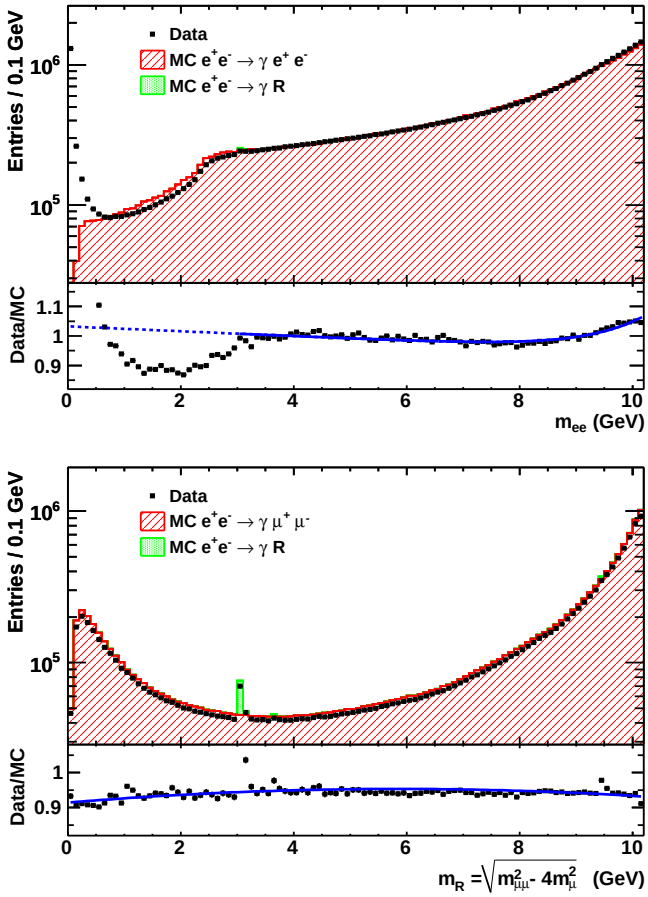

FIG. 1: Distribution of the final dielectron (top) and reduced dimuon invariant masses (bottom), together with the predictions of various simulated SM processes and ISR production of $J/\psi, \psi(2S)$, $\Upsilon(1S)$, and $\Upsilon(2S)$ resonances (collectively labeled as R). The fit to the ratio between data and simulated events is described in the text.

cumulative mass distributions [36]. An uncertainty of 5%-10% in this procedure is assessed by taking the next-to-closest instead of the closest simulated mass points to interpolate the signal shape. Samples of simulated and reconstructed $e^+e^- \to \gamma J/\psi, J/\psi \to l^+l^-$ events indicate that the simulation underestimates the signal width by 8% (4%) for the dielectron (dimuon) channel. We assume that this difference is independent of the dark photon mass, and we increase the signal pdf width by the corresponding amount for all mass hypotheses. We propagate half of these correction factors as systematic uncertainties on the fitted signal yields.

The radiative Bhabha background below 0.1 GeV is described by a fourth order polynomial, and elsewhere by a third order polynomial. The radiative dimuon background is parametrized by a third order polynomial, constrained to pass through the origin for fits in the region below 0.05 GeV. Peaking contributions from the J/ψ, $\psi(2S)$, $\Upsilon(1S)$, and $\Upsilon(2S)$ resonances for both final states are included where appropriate. Their shapes are modeled as Crystal Ball or Gaussian functions with parameters extracted from fits to the corresponding Monte Carlo samples. Similarly to the signal pdf, we increase their width by 8% (4%) for the dielectron (dimuon) final states. The interference between vector resonances with radiative dilepton production is observed for the ω and ϕ mesons, and is fit with the following empirical function:

$$f(m) = (a+bm+cm^2+dm^3)\left|1 - Q\frac{m_{\omega/\phi}\Gamma}{s - m^2_{\omega/\phi} - im_{\omega/\phi}\Gamma}\right|^2$$

where $m_{\omega/\phi}$ (Γ) denotes the mass (width) of the resonance, Q the resonant fraction, and a, b, c, d are free parameters. We fix the masses and widths to their nominal values [37], and let their fractions float. We exclude the resonant regions from the search, vetoing ranges of ± 30 MeV around the nominal mass of the ω and ϕ resonances, and ± 50 MeV around the J/ψ, $\psi(2S)$, and $\Upsilon(1S, 2S)$ resonances (approximately $\pm 5\sigma_R$, where σ_R denotes the experimental resolution of the resonances). An alternative signal extraction fit, using parametric pdfs for signal [21] and a different background parametrization has been performed for the $\mu^+\mu^-$ channel. The results of both methods are statistically consistent with each other. The uncertainty on the background modeling is estimated by using an alternative description of the radiative Bhabha and dimuon contributions based on a second or fourth order polynomial, depending on the mass hypothesis. This uncertainty is almost as large as the statistical uncertainty near the dielectron threshold, and can be as large as 50% of the statistical uncertainty in the vicinity of the $\Upsilon(1S, 2S)$ resonances. Outside these regions, the uncertainty varies from a few percent at low masses to $\sim 20\%$ of the statistical uncertainty in the high mass region. In addition we propagate half of the corrections applied to the signal width, as well as the uncertainties on the ω and ϕ masses and widths, as systematic uncertainties on the fitted signal yields.

The $e^+e^- \to \gamma A', A' \to e^+e^-$ and $e^+e^- \to \gamma A', A' \to \mu^+\mu^-$ cross-sections as a function of the dark photon mass are obtained by combining the signal yields of each data sample, divided by the efficiency and luminosity. The cross-sections as a function of $m_{A'}$ are shown in Fig. 2; the distributions of the statistical significances of the fits are displayed in Fig. 3. The statistical significance of each fit is taken as $\mathcal{S} = \sqrt{2\log(\mathcal{L}/\mathcal{L}_0)}$, where $\mathcal{L}$ and $\mathcal{L}_0$ are the likelihood values for fits with a free signal and the pure background hypothesis, respectively. We estimate trial factors by generating a large sample of Monte Carlo experiments. The largest local significance is 3.4σ (2.9σ), observed near $m_{A'} = 7.02$ GeV (6.09 GeV) for the dielectron (dimuon) final state. Including trial factors, the corresponding p-value is 0.57 (0.94), consistent with the null hypothesis.

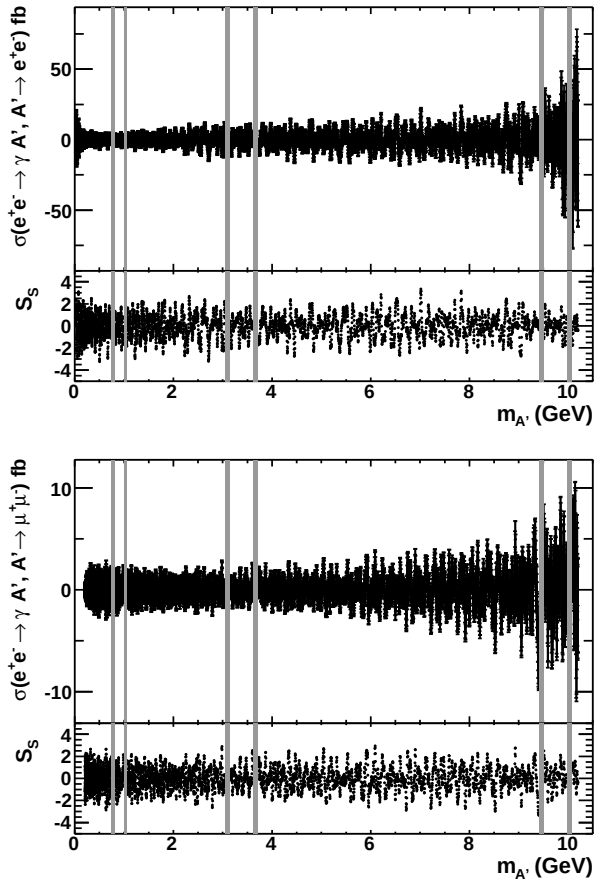

FIG. 2: The $e^+e^- \to \gamma A', A' \to e^+e^-$ (top) and $e^+e^- \to \gamma A', A' \to \mu^+\mu^-$ (bottom) cross-sections together with their respective statistical significance (S_S) as a function of the dark photon mass. The gray bands indicate the mass regions that are excluded from the analysis.

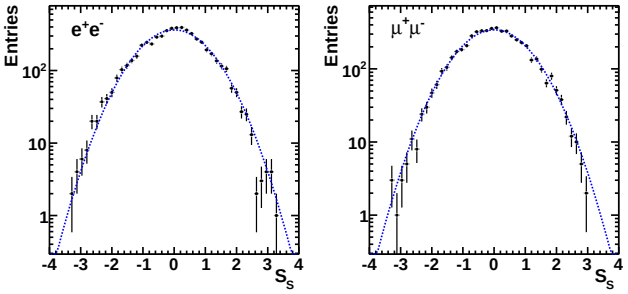

FIG. 3: Distribution of the statistical significance (S_S) from the fits to the dielectron (left) and dimuon (right) final states, together with the expected distribution for the null hypothesis (dashed line).

We extract the $e^+e^- \to \gamma A'$ cross-section for each final state using the expected dark photon branching fractions $A' \to l^+l^-$ from Ref. [9], and combine the results into a single measurement. The uncertainties on the dark photon branching fractions (0.1%-4%), the luminosity (0.6%), and the limited Monte Carlo statistics (0.5-4%) are propagated as systematic uncertainties. We derive 90% confidence level (CL) Bayesian upper limits on the $e^+e^- \to \gamma A'$ cross-section, assuming a flat prior for the cross-section. The limits are typically at the level of $\mathcal{O}(1-10)$ fb. These results are finally translated into 90% CL upper limits on the mixing strength between the photon and dark photon as a function of the dark photon mass [10]. The results are displayed in Fig. 4. The average correlation between neighboring points is around 90%. Bounds at the level of $10^{-4} - 10^{-3}$ for $0.02\,\text{GeV} < m_{A'} < 10.2\,\text{GeV}$ are set, significantly improving previous constraints derived from beam-dump experiments [11, 12, 18], the electron anomalous magnetic moment [13], KLOE [14, 15], WASA-at-COSY [16], HADES [17], A1 at MAMI [19], and the test run from APEX [20]. These results also supersede and extend the constraints based on a search for a light *CP*-odd Higgs boson at *BABAR* [21, 22] with a smaller dataset. No signal consistent with the excess reported by the HyperCP experiment close to 214 MeV is observed [38, 39]. We further constrain the range of the parameter space favored by interpretations of the discrepancy between the calculated and measured anomalous magnetic moment of the muon [39]. The remaining mass region of allowed parameters, $15\,\text{MeV} \lesssim m_{A'} \lesssim 30\,\text{MeV}$ will be probed by several planned experiments in the near future (see for example ref. [1] for a discussion).

In conclusion, we have performed a search for dark photon production in the range $0.02\,\text{GeV} < m_{A'} < 10.2\,\text{GeV}$. No significant signal has been observed and upper limits on the mixing strength ϵ at the level of $10^{-4} - 10^{-3}$ have been set. These bounds significantly improve the current constraints, and exclude almost all of the remaining region of the parameter space favored by the discrepancy between the calculated and measured anomalous magnetic moment of the muon.

ACKNOWLEDGMENTS

The authors wish to thank Rouven Essig and Sarah Andreas for providing us the constraints derived from existing experiments. We also thank Rouven Essig, Philip Schuster and Natalia Toro for useful discussions and for providing us with their MadGraph code to simulate dark photon processes. We are grateful for the excellent luminosity and machine conditions provided by our PEP-II colleagues, and for the substantial dedicated effort from the computing organizations that support *BABAR*. The collaborating institutions wish to thank SLAC for its support and kind hospitality. This work is supported by DOE and NSF (USA), NSERC (Canada), CEA and

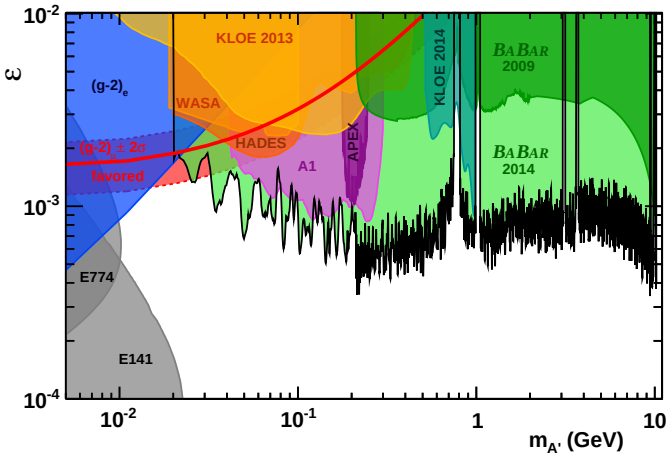

FIG. 4: Upper limit (90% CL) on the mixing strength ϵ as a function of the dark photon mass. The values required to explain the discrepancy between the calculated and measured anomalous magnetic moment of the muon [39] are displayed as a red line.

CNRS-IN2P3 (France), BMBF and DFG (Germany), INFN (Italy), FOM (The Netherlands), NFR (Norway), MES (Russia), MICIIN (Spain), STFC (United Kingdom). Individuals have received support from the Marie Curie EIF (European Union), the A. P. Sloan Foundation (USA) and the Binational Science Foundation (USA-Israel).

* Now at the University of Tabuk, Tabuk 71491, Saudi Arabia
† Also with Università di Perugia, Dipartimento di Fisica, Perugia, Italy
‡ Now at Laboratoire de Physique Nucléaire et de Hautes Energies, IN2P3/CNRS, Paris, France
§ Now at the University of Huddersfield, Huddersfield HD1 3DH, UK
¶ Deceased
** Now at University of South Alabama, Mobile, Alabama 36688, USA
†† Also with Università di Sassari, Sassari, Italy
‡‡ Also with INFN Sezione di Roma, Roma, Italy
§§ Now at Universidad Técnica Federico Santa Maria, Valparaiso, Chile 2390123

[1] See for example R. Essig, J. A. Jaros, W. Wester, P. H. Adrian, S. Andreas, T. Averett, O. Baker and B. Batell *et al.*, arXiv:1311.0029 [hep-ph], and references therein.
[2] B. Holdom, Phys. Lett. B **166**, 196 (1986).
[3] D. P. Finkbeiner and N. Weiner, Phys. Rev. D **76**, 083519 (2007).
[4] M. Pospelov, A. Ritz, and M. B. Voloshin, Phys. Lett. B **662**, 53 (2008).
[5] N. Arkani-Hamed, D. P. Finkbeiner, T. R. Slatyer, and N. Weiner, Phys. Rev. D **79**, 015014 (2009).
[6] O. Adriani *et al.* [PAMELA Collaboration], Nature **458**, 607 (2009).
[7] M. Ackermann *et al.* [Fermi LAT Collaboration], Phys. Rev. Lett. **108**, 011103 (2012).
[8] M. Aguilar *et al.* [AMS Collaboration], Phys. Rev. Lett. **110**, 141102 (2013).
[9] B. Batell, M. Pospelov, and A. Ritz, Phys. Rev. D **79**, 115008 (2009).
[10] R. Essig, P. Schuster, and N. Toro, Phys. Rev. D **80**, 015003 (2009).
[11] J. Blumlein and J. Brunner, Phys. Lett. B **701** 155 (2011).
[12] S. Andreas, C. Niebuhr and A. Ringwald, Phys. Rev. D **86**, 095019 (2012).
[13] M. Endo, K. Hamaguchi and G. Mishima, Phys. Rev. D **86**, 095029 (2012).
[14] D. Babusci *et al.* [KLOE-2 Collaboration], Phys. Lett. B **720**, 111 (2013).
[15] D. Babusci *et al.* [KLOE-2 Collaboration], Phys. Lett. B **736**, 459 (2014).
[16] P. Adlarson *et al.* [WASA-at-COSY Collaboration], Phys. Lett. B **726**, 187 (2013).
[17] G. Agakishiev *et al.* [HADES Collaboration], Phys. Lett. B **731**, 265 (2014).
[18] J. Blmlein and J. Brunner, Phys. Lett. B **731** 320 (2014).
[19] H. Merkel, P. Achenbach, C. A. Gayoso, T. Beranek, J. Bericic, J. C. Bernauer, R. Boehm and D. Bosnar *et al.*, Phys. Rev. Lett. **112**, 221802 (2014).
[20] S. Abrahamyan *et al.* [APEX Collaboration], Phys. Rev. Lett. **107**, 191804 (2011).
[21] B. Aubert *et al.* [*BABAR* Collaboration], Phys. Rev. Lett. **103**, 081803 (2009).
[22] J. D. Bjorken, R. Essig, P. Schuster and N. Toro, Phys. Rev. D **80**, 075018 (2009).
[23] B. Aubert *et al.* [*BABAR* Collaboration], arXiv:0908.2821 [hep-ex].
[24] J. P. Lees *et al.* [*BABAR* Collaboration], Phys. Rev. Lett. **108**, 211801 (2012).
[25] B. Aubert *et al.* [*BABAR* Collaboration], Nucl. Instrum. Meth. A **479**, 1 (2002).
[26] B. Aubert *et al.* [*BABAR* Collaboration], Nucl. Instrum. Meth. A **729**, 615 (2013).
[27] J. P. Lees *et al.* [*BABAR* Collaboration], Nucl. Instrum. Meth. A **726**, 203 (2013).
[28] Natural units ($\hbar = c = 1$) are used throughout this paper.
[29] J. Alwall, P. Demin, S. de Visscher, R. Frederix, M. Herquet, F. Maltoni, T. Plehn, and D. L. Rainwater *et al.*, JHEP **0709**, 028 (2007).
[30] S. Jadach, W. Placzek and B. F. L. Ward, Phys. Lett. B **390**, 298 (1997).
[31] S. Jadach, B. F. L. Ward and Z. Was, Phys. Rev. D **63**, 113009 (2001).
[32] A. B. Arbuzov *et al.*, J. High Energy Phys. **9710**, 001 (1997).
[33] M. Caffo, H. Czyż, and E. Remiddi, Nuovo Cim. **A110**, 515 (1997); Phys. Lett. **B327**, 369 (1994).
[34] S. Agostinelli *et al.* (GEANT4 Collab.), Nucl. Instrum. Methods Phys. Res., Sect. A **506**, 250 (2003).
[35] See Supplemental Material at [url] for example of fits to the data and additional plots on the limits on $e^+e^- \to \gamma A', A' \to l^+l^-$ cross-sections.
[36] A. L. Read, Nucl. Instrum. Meth. A **425**, 357 (1999).
[37] J. Beringer *et al.* (Particle Data Group), Phys. Rev. **D 86**, 010001 (2012) and 2013 partial update for the 2014

edition.
[38] H. Park *et al.* [HyperCP Collaboration], Phys. Rev. Lett. **94**, 021801 (2005).
[39] M. Pospelov, Phys. Rev. D **80**, 095002 (2009).